Application of Near-Infrared Luminescence Spectroscopy to Vanadium(III) Complexes. Characterization of their Electronic Ground State

*Rémi Beaulac, Jean Christophe Tremblay, Guillaume Bussière and Christian Reber**

Contribution from: Département de chimie, Université de Montréal, C.P. 6128, Succ. Centre-ville, Montréal, Québec H3C 3J7, Canada

Received: December 20, 2001

Accepted: (in revised form) February 22, 2002

Résumé

La spectroscopie de luminescence dans le proche-infrarouge constitue un outil de choix pour la caractérisation détaillée de la structure électronique de l'état fondamental ($^3T_{1g}$ en symétrie O_h) des complexes du vanadium(III). Les spectres de luminescence à basse température de $[V(urée)_6]I_3$, de $[VCl_6]^{3-}$ dopé dans Cs_3AlCl_6 et de $[V(H_2O)_6]^{3+}$ dans une série d'aluns dopés sont présentés. Dans tous les cas, la transition de luminescence de plus haute énergie observée se situe entre 9400 cm^{-1} et 10500 cm^{-1} sous la forme de bandes étroites; des transitions électroniques ainsi que des progressions vibroniques apparaissent à des énergies aussi faibles que 8000 cm^{-1}. L'état fondamental du complexe $[V(urée)_6]^{3+}$ est scindé en deux composantes trigonales, séparées de 1400 cm^{-1} l'une de l'autre, une séparation plus large que celle observée dans le cas de $Al_2O_3:V^{3+}$, un complexe dont la distorsion trigonale du fragment VO_6 est pourtant nettement plus importante que dans le complexe $[V(urée)_6]^{3+}$. Comparativement, le complexe $[VCl_6]^{3-}$ possède une séparation trigonale de 1000 cm^{-1}. Des calculs basés sur la théorie du champ des ligands ainsi que sur la fonctionnelle de la densité ont été effectués pour interpréter les résultats spectroscopiques. Les transitions de luminescence des aluns de vanadium(III) se situent autour de 10199 ± 15 cm^{-1} et se déplacent vers une énergie plus haute de 34 cm^{-1} pour les cristaux deutérés.

*Author to whom correspondence should be addressed. E-mail: reber@chimie.umontreal.ca

Abstract

Near-infrared luminescence spectra of vanadium(III) complexes often allow a direct observation of the energy differences between levels of the electronic ground state ($^3T_{1g}$ in O_h symmetry). Low-temperature spectra are reported for $[V(urea)_6]I_3$, for $[VCl_6]^{3-}$ doped into Cs_3AlCl_6 and for $[V(H_2O)_6]^{3+}$ in a series of doped alums. The highest energy luminescence transitions in all spectra occur as sharp transitions between 9400 cm^{-1} and 10500 cm^{-1}, and lower energy vibronic and electronic transitions are observed at energies as low as 8000 cm^{-1}. The ground state of the $[V(urea)_6]^{3+}$ complex is split into two trigonal components separated by 1400 cm^{-1}. This separation is larger than the corresponding energy difference reported for $Al_2O_3:V^{3+}$, even though the VO_6 fragment in $[V(urea)_6]^{3+}$ is much closer to octahedral symmetry than in the doped oxide lattice. $[VCl_6]^{3-}$ in the doped chloride lattice shows a separation of approximately 1000 cm^{-1}. Ligand field and density functional calculations are used to rationalize this observation. The highest energy luminescence origin is observed at 10199 ± 15 cm^{-1} in the doped alums and it shifts to higher energy by 34 cm^{-1} upon deuteration.

Key words: Near-infrared luminescence spectroscopy, vanadium(III) complexes.

Introduction

Molecular coordination compounds containing metal centers with the d^2 electron configuration, such as vanadium(III) and titanium(II), are of current interest in two research areas: for near-

infrared to visible upconversion (1) and for the detailed determination of the electronic structure of molecular crystals (2,3). The near-infrared luminescence spectra of these complexes are of fundamental importance to both domains. In this report, we present spectra with qualitative similarities for a series of approximately octahedral vanadium(III) complexes.

The first area, near-infrared to visible upconversion (1), has recently been explored for d^2 configured ions doped into chloride host lattices (4). The structure of the host material has an important influence on these optical processes, as was illustrated by the comparison of the NaCl and $MgCl_2$ lattices (4,5), underlining the need for precise determinations of energy differences between electronic states through near-infrared luminescence spectroscopy. Of key importance for the design of such optical materials are the low-energy electronic states in the near-infrared wavelength range, traditionally neglected in spectroscopic studies because of the limitations of routine instruments. One of the goals of this report is to characterize such states for a variety of compounds and to explore the variation of luminescence energies and bandshapes for vanadium(III) complexes.

The second area of interest concerns the interaction between metal-centered electronic states and features of the ligand environment in molecular solids containing transition metal compounds. A well known example of such interactions are transition metal alums, where the orientation of aquo ligands is often determined by the hydrogen bonding network throughout the crystal, leading to large energy separations of levels arising from a degenerate ground state in idealized octahedral symmetry. The electronic structure of the ground state has recently been probed by EPR, electronic Raman and absorption spectroscopy for the $[V(H_2O)_6]^{3+}$ complex in alum lattices (2,3). We show in the following that near-infrared luminescence spectroscopy has become a technique that can contribute complementary experimental information to the characterization of such molecular compounds, even if the luminescence intensities are very weak.

Six-coordinate vanadium(III) complexes have their lowest energy excited states in the near-infrared region between 970 nm and 1100 nm. Luminescence measurements for a wide variety of compounds have become possible with highly sensitive detectors and efficient microscope optics. In the literature, only spectra for solids with high quantum yields, such as the cubic elpasolite Cs_2NaYCl_6 doped with V^{3+} (6), or partial spectra at the high energy limit of the near-infrared region (7-10), have been reported, leading to very limited knowledge of observable luminescence phenomena for vanadium(III) complexes.

In the following, we present new luminescence spectra of $V(urea)_6I_3$, of $[VCl_6]^{3-}$ doped into Cs_3AlCl_6 and of $[V(H_2O)_6]^{3+}$ in a series of doped alums. The results show that even disordered solids and aqua complexes can be characterized by near-infrared luminescence spectroscopy, a technique that has become a powerful, general tool for inorganic and materials chemistry.

Experimental

$V(urea)_6I_3$ was prepared by dissolving V_2O_3 (Aldrich) in warm 2M H_2SO_4. A stoichiometric amount [6 :1 with respect to the concentration of vanadium(III)] of urea was then added to the solution, followed by a small excess of potassium iodide. The solution was allowed to evaporate in a desiccator under argon for a few days. $V(urea)_6I_3$ crystallizes as green crystals in the R_{3c}- space group (11). The green crystals become yellow over a few weeks, indicating a change in the chemical structure of the compound. All results reported in the following were obtained with green crystals.

Cs_3AlCl_6 doped with V^{3+} was prepared by dissolving a 1:5 ratio of aluminum chloride hydrate $AlCl_3{\cdot}6H_2O$ and vanadium(III) chloride hydrate $VCl_3.6H_2O$ (Aldrich) in a minimal amount of warm water. The liquid is then evaporated in a desiccator. The resulting compound is dissolved in 9M HCl and placed in a desiccator under HCl atmosphere. A crystalline mauve product, the typical color of $[VCl_6]^{3-}$ (6), was obtained in minority after a few weeks among a majority of green crystals.

The alum $GuV(SO_4)_2{\cdot}12H_2O$, where Gu denotes the guanidinium cation (GuH = $H_2NCNHNH_2$), was prepared following a recent literature report (3). $RbGa(SO_4)_2.12H_2O$ doped with V^{3+} was synthesized by heating a 1M solution of VCl_3 (Aldrich) in 3M H_2SO_4. A solution of Rb_2SO_4 (1.5M, Aldrich) and $Ga_2(SO_4)_3.xH_2O$ (0.5 M) was then added to the solution of the vanadium salt and put in the refrigerator for a few days. The vanadium(III) compound which precipitated quantitatively from the solution was recrystallized from a minimal amount of warm 6M H_2SO_4. $NH_4V(SO_4)_2.12H_2O$ was prepared from a 0.5M solution of V_2O_3 in 6M H_2SO_4. Concentrated ammonia (28% NH_3 in water) was

added until a brown precipitate began to appear. After a few days in the refrigerator, small purple-blue crystals were obtained in addition to a green precipitate. The purple crystals were collected and put back into the filtered solution to obtain crystals of sufficient size for spectroscopy.

Two different instruments were used to obtain luminescence spectra from the complexes. Luminescence at wavelengths shorter than 1050 nm was measured using the Raman system described below. Emission at longer wavelengths was dispersed through a 0.5m monochromator (Spex 500M) and detected with a Hamamatsu R5509-72 photomultiplier cooled to –80°C. The photocurrent was amplified with a fast response pre-amplifier (Stanford Research SR445) and collected with a photon counter (Stanford Research SR400). The spectra reported here were not corrected for system response, because the sensibility of our instruments varies by less than 10% over the wavelength range examined.

Raman spectra were measured using a Renishaw System 3000 Raman imaging microscope. The microscope was used to focus the laser light onto a spot approximately 1 μm in diameter and to collect the scattered light. The 514.5 nm excitation line of an Ar^+ ion laser was used the excitation source. The appropriate Renishaw notch filter allows measurements of Raman shifts larger than 100 cm^{-1}. The back scattered Raman light was detected with a Peltier cooled CCD detector. Samples were cooled with a Linkam THMS 600 cryostat using liquid nitrogen. Low-temperature absorption spectra were measured with a Varian Cary 5E spectrometer. The sample temperature was controlled with an Oxford Instruments CF-1204 He gas flow cryostat.

Spectroscopic results

Figure 1 shows luminescence spectra of $V(urea)_6I_3$ at different temperatures. The most prominent feature of all spectra is a sharp line at 9928 cm^{-1} (25 K), readily assigned as an electronic origin, in agreement with a previous assignment on the perchlorate salt of this complex (7). This origin shifts to 9922 cm^{-1} at 80 K and to 9897 cm^{-1} at 200 K. The luminescence spectrum shows a number of lower-energy transitions corresponding to electronic and vibronic transitions to ground-state levels. Their energy differences from the highest-energy luminescence transition are summarized in Table I and are discussed in detail in the following section.

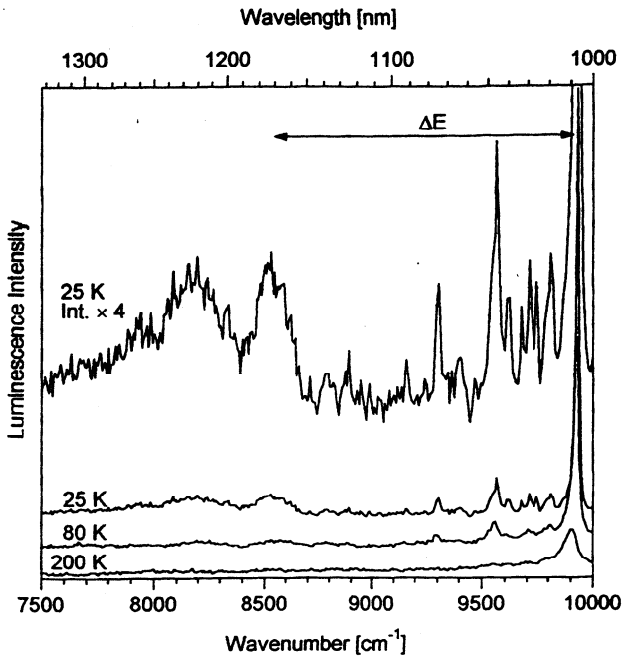

Figure 1. Low-temperature luminescence spectra of $V(urea)_6I_3$. The energy difference ΔE denotes the splitting of the electronic ground state.

A broad band is observed approximately 1400 cm^{-1} lower in energy than the prominent origin at 9928 cm^{-1}. Based on the luminescence and Raman spectra presented in the following, this band is assigned to the transition from the emitting state to the higher-energy component of the electronic ground state. To our knowledge, this is the first report of a full luminescence spectrum for the $[V(urea)_6]^{3+}$ complex. The previously published partial spectrum of the perchlorate salt (7) contains only the highest energy transition at 9895 cm^{-1} and reports a 6 cm^{-1} splitting of this band, corresponding to the zero-field splitting between the lowest energy ground state levels. The resolution of the $V(urea)_6I_3$ spectra presented here does not allow us to determine this energy difference.

The Raman spectrum of $V(urea)_6I_3$ is presented in Figure 2. All vibrational energies are given in Table I. An important feature of this spectrum is the presence of a broad band with a strong temperature dependence, shown in the inset to Figure 2. This band is assigned to an electronic Raman transition between electronic ground state levels, in quantitative agreement with the results obtained from luminescence spectroscopy, as shown in Figure 3. In this figure, the origin of the axis defining the Raman shift is aligned to coincide with the origin of

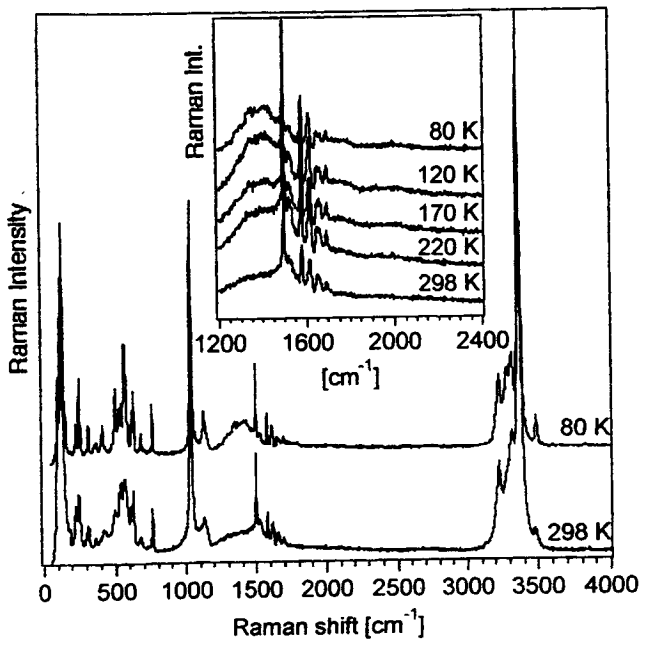

Figure 2. Raman spectra of $V(urea)_6I_3$. The inset shows the detailed temperature dependence in the region of the electronic Raman transition.

Table I. Vibrational frequencies for $V(urea)_6I_3$ from Raman and luminescence spectra. Assignments indicate regions in which these modes occur, not specific peaks in the spectra.

Frequency [cm^{-1}]	Assignment
3486[a]	
3364 – 3326[a]	ν N-H
1692[a]	
1650[a]	δ N-H
1577[a]	ν_{as} C-O
1495[a]	ν_{as} C-N
1125[a]	ν_{as} C-O
1036[a]	ν_s C-N
760[a]	
680[a]	
628-616[a]	δ N-C-O
624[b]	
565[a]	
540[a]	δ N-C-N
526[a]	
501[a]	
412[a]	
362[a, b]	
312[a]	ν V-O
250[a]	
225[a]	
151[a]	
131[a]	
100[a]	

[a] Raman [b] Luminescence

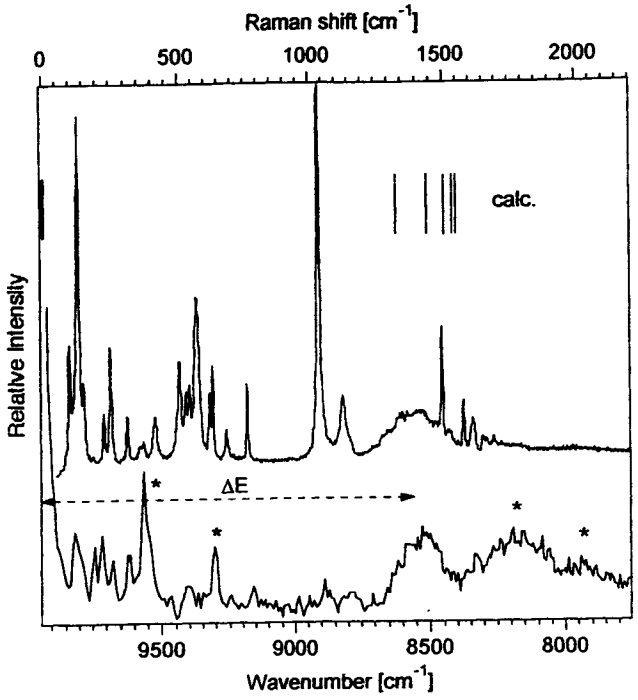

Figure 3. Comparison of the luminescence spectrum at 25 K (lower trace, bottom abscissa) and the Raman spectrum at 80 K (upper trace, top abscissa) for $V(urea)_6I_3$. Both the top and bottom wavenumber axes span a range of 2200 cm^{-1}. The energy difference ΔE denotes the splitting of the electronic ground state, observable in both the luminescence and Raman spectra. The splitting of the ground state due to low symmetry and spin-orbit coupling is given by the vertical bars above the spectra. Asterisks denote two vibronic bands that are intense in the luminescence spectrum and observed lower in energy by 362 cm^{-1} and 624 cm^{-1} than their corresponding electronic origins.

the luminescence spectrum and the top and bottom axes cover the same wavenumber range of 2200 cm^{-1}, showing the exact superposition of vibrational bands and the broad electronic transition in both spectra. The comparison of luminescence and Raman spectra allows us to identify the vibrational frequencies of 362 cm^{-1} and 624 cm^{-1} (denoted by asterisks in Figure 3) that are more intense in the luminescence spectra than in the Raman spectrum. They are observed on the low-energy side of both sets of electronic origins and most likely are vibronic origins, expected for centrosymmetric complexes. Other bands are clearly more intense in the Raman spectrum and correspond to gerade parity modes of centrosymmetric complexes.

Figure 4 shows the luminescence spectrum of Cs_3AlCl_6 doped with V^{3+}. This doped system is likely to contain a variety of luminophores, but the spectra in Figure 4 are nevertheless well resolved and qualitatively similar to the spectra in Figure 1,

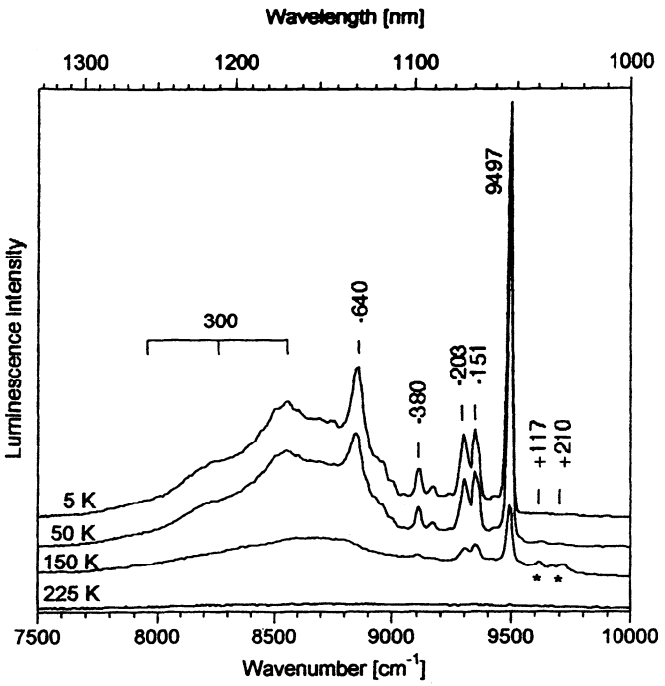

Figure 4. Low-temperature luminescence spectra of $Cs_3[AlCl_6]:V^{3+}$. The wavenumber axis is identical to Figure 1. Asterisks denote hot bands. All energy intervals are given in wavenumber units, differences are given relative to the origin at 9497 cm^{-1}.

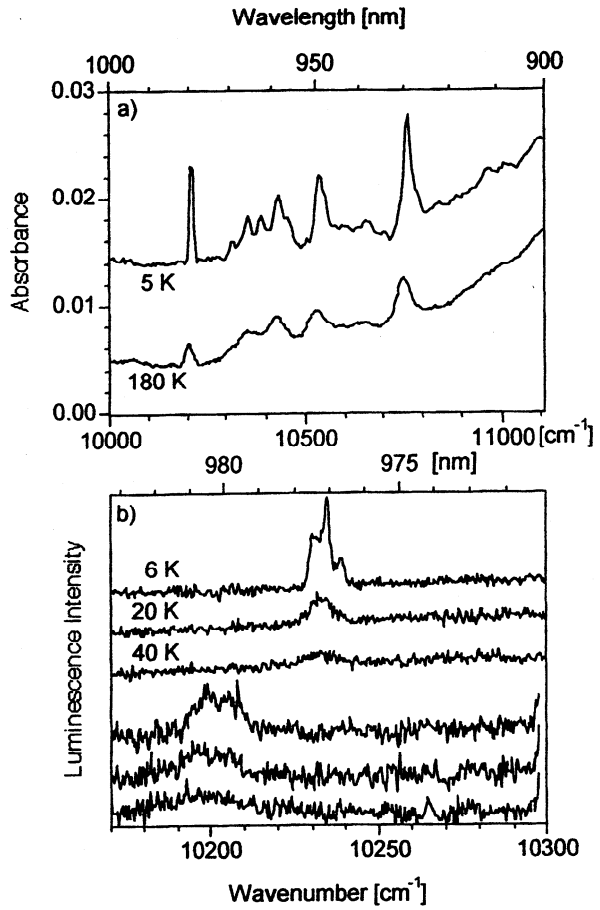

Figure 5. (a) Low-temperature absorption spectra of $RbV(SO_4)_2{\cdot}12H_2O$ in the region of the lowest energy electronic transition. (b) Luminescence spectra of different alums of vanadium(III). Top to bottom: $CsAl(SO_4)_2{\cdot}12D_2O{:}V(D_2O)_6^{3+}$ at three different temperatures, $GuV(SO_4)_2{\cdot}12H_2O$, $RbV(SO_4)_2{\cdot}12H_2O$, $NH_4V(SO_4)_2{\cdot}12H_2O$.

which also show a dominant high-energy origin and a broad band at lower energy, indicating a split electronic ground state. The highest energy luminescence transition is observed at 9497 cm^{-1}, and it shifts by less than 2 cm^{-1} between 5 K and 225 K, in contrast to the $[V(urea)_6]^{3+}$ complex, where a larger shift of approximately 130 cm^{-1} is observed between 25 K and 200 K. This transition is slightly lower in energy than the origin reported at 9620 cm^{-1} for a doped chloride lattice with perfect octahedral coordination geometry (6). It most likely arises from a hexachloro complex, even though the crystals were grown from aqueous solution. The lowest-energy origin observed for the mixed aquo-chloro complex *trans*-$[VCl_2(H_2O)_4]^+$ occurs at 9717 cm^{-1} (12), higher in energy than the literature reports for $[VCl_6]^{3-}$ (6,13). The origins of $[V(H_2O)_6]^{3+}$ are even higher in energy, as illustrated in Figure 5. At high temperatures, vibrational hot bands, denoted by asterisks in Figure 4, are observed at energies higher by 123 cm^{-1} and 222 cm^{-1} than the prominent origin.

The broad band seen at approximately 1150 nm in Figure 4 shows that the exact symmetry of $[VCl_6]^{3-}$ is not perfectly octahedral and we estimate from the figure that the ground state splitting is on the order of 1000 cm^{-1}. The shoulders observed on the broad band between 8700 cm^{-1} and 8000 cm^{-1} are separated by 300 cm^{-1}, an energy close to the totally symmetric V-Cl stretching mode, observed at 294 cm^{-1} in Cs_2NaYCl_6 (6). The series of bands is likely to correspond to a vibronic progression specific to the higher-energy ground state components. No such progression is observed on the intense origin at 9497 cm^{-1}, indicating an important difference from $V[(urea)_6]^{3+}$, where corresponding vibronic origins are observed on both the narrow and large electronic bands. We note that no broad luminescence band from a higher excited state is observed, in contrast to $Cs_2NaYCl_6{:}V^{3+}$ and other doped centrosymmetric chloride lattices, where a broad emission band dominates at temperatures above 100 K (6,13).

$[VCl_6]^{3-}$ doped into all chloride lattices examined in the literature has a ground-state splitting of less than 500 cm^{-1}, lower by more than a factor of two than observed in Figure 4.

Figure 5a shows the lowest-energy transition in the absorption spectra of $RbV(SO_4)_2 \cdot 12H_2O$ at two temperatures. The electronic origin is observed at 10212 cm^{-1}. This energy is in good agreement with the position of 10199 ± 15 cm^{-1} for the weak transition in the luminescence spectrum of the same compound, shown in Figure 5b. Luminescence spectra of some other alums of vanadium(III) are included for comparison in Figure 5b. The very low luminescence intensity is due to the high-frequency modes of the ligands, but luminescence spectra can be observed and allow us to determine precise emitting state energies and effects of deuteration, such as the 34 cm^{-1} shift to higher energy for the deuterated alum compared to the aquo crystals, a comparison illustrated in Figure 5b.

We attempted to observe luminescence from $Cs_3VCl_6.12\ X_2O$ (X : H or D), containing *trans*-$VCl_2(X_2O)_4^+$ chromophores. The position of their lowest energy electronic transition is known from absorption spectroscopy as 9717 cm^{-1} (12), significantly lower in energy than for the alums in Figure 5 and below the lower wavelength limit of the CCD detector used with the microscope. In spite of the high sensibility of the equipment used to obtain the spectra in Figures 1 and 4, we were not able to observe any signal.

Luminescence spectra define the energy of the emitting state for all three complexes studied here. This quantity is directly available from the experimental spectra and cannot be determined by Raman or EPR spectroscopy. Further information can be derived from the spectra by using theoretical models, as shown in the following section.

Discussion

The near-infrared luminescence spectra in Figures 1, 3- 5 show that well resolved transitions can be measured for a wide variety of vanadium(III) complexes with polyatomic ligands. The most important quantities provided by luminescence spectra are ground state properties: electronic and vibrational energies. The simplest situation occurs for exactly octahedral complexes with monoatomic ligands, such as $[VCl_6]^{3-}$ units in the doped elpasolite $Cs_2NaCl_6:V^{3+}$ (6). Their electronic ground state in O_h point group symmetry is $^3T_{1g}$ and low-temperature emission is observed from the $^1T_{2g}$ state arising from the same electron configuration as the ground state. The resulting luminescence spectra correspond to well-resolved spin-flip transitions, observed for a variety of compounds containing ions with the d^2 electron configuration (6,13,14) and illustrated schematically in the left-hand column of Figure 6. Spin-orbit coupling separates the $^3T_{1g}$ state into the levels illustrated in the middle column of Figure 6. The energies given in the Figure were determined for an octahedral chloride complex in the literature (6). Lowest in energy are the E_g and T_{2g} levels, degenerate in first order and separated by less than 10 cm^{-1} in experimental spectra (6). They are approximately 130 cm^{-1} lower in energy than the T_{1g} level, which is approximately 60 cm^{-1} below the A_{1g} level. This 2:1 (130 cm^{-1} : 60 cm^{-1}) pattern of the energy intervals corresponds well to the Landé pattern expected in first order. The main luminescence intensity of this and other centrosymmetric chromophores (6,13,14) is contained in vibronic origins.

The ground state for the vanadium(III) complexes studied here does not correspond to this simple splitting pattern, as even small deviations from exact octahedral point group symmetry lead to energy differences between levels arising from the $^3T_{1g}$ (O_h) ground state that are much larger than the separations of spin-orbit levels discussed above. Spectra illustrating this have been reported for V^{3+} doped into Al_2O_3 and for the isoelectronic Ti^{2+} ion doped into $MgCl_2$ and they show ground state splittings of 1100 cm^{-1} and 750 cm^{-1}, respectively (14,15). Our spectra allow us to determine these energy separations for complexes with molecular ligands. For the trigonal complex $[V(urea)_6]^{3+}$ studied here, the energy levels are shown in the right-hand column of Figure 6. Vibronic origins are less prominent in these spectra, because the exact molecular symmetry is often not centrosymmetric, relaxing the symmetry restrictions and leading to significant intensity for the electronic origins.

The full luminescence spectrum for $V(urea)_6I_3$ in Figure 1 allows us to characterize the ground state in detail. The highest energy transition observed for this complex occurs at 9928 cm^{-1} and is sharp. Figure 1 shows a broader band at significantly lower energy, corresponding to the electronic transition from the emitting state to the higher-energy ground state components. This separation is an important characteristic and a direct measure for the energetic consequences of the structural deviations from

octahedral symmetry. For $V(urea)_6I_3$, it is on the order of 1500 cm^{-1}, as indicated in Figures 1 and 3. This is significantly higher than the value of approximately 1100 cm^{-1} determined for V^{3+} doped into Al_2O_3 (15), the only other luminescence reported from a trigonal vanadium(III) luminophore with six oxygen ligator atoms. It is interesting to note that the Raman spectrum shows a single broad band for the electronic transition, but the luminescence spectrum shows two additional lower energy transitions with maxima at approximately 8200 cm^{-1} and 7950 cm^{-1}, not observed in the Raman spectrum. The energy differences between these broad luminescence bands correspond well to the difference between the highest energy luminescence transition and the most intense vibronic origins, identified in the preceding section and in Figure 3 from the comparison of luminescence and Raman spectra. This comparison illustrates clearly the spectroscopic differences between luminescence and electronic Raman transitions. Polarized low-temperature single-crystal absorption spectra of $V(urea)_6I_3$ have been reported (16), but they do not show enough resolution to precisely determine splittings of triplet excited states. Only unresolved broad bands are observed, much more fallible experimental quantities for the determination of energy separations than the luminescence and electronic Raman spectra used here.

The energy differences between electronic states of $V[(urea)_6]^{3+}$ can be analyzed with theoretical models using the known molecular structure of this complex. All models are compared to the experimental transition energies observed in luminescence, Raman and absorption spectra. The standard approach involves ligand field theory. We use the angular overlap (AOM) formalism as implemented in the AOMX program (17), because it is easily adapted to any given molecular structure. The angles θ and ϕ used to describe all six vanadium – oxygen bonds (18) are derived from crystallographic data (11). The θ values are smaller by less than one degree than the angles of 54.7° and 125.3° for a perfectly octahedral coordination geometry, corresponding to a slight trigonal compression of the VO_6 fragment in $V[(urea)_6]^{3+}$. This trigonal distortion is significantly smaller than for the oxygen coordination environment of V^{3+} doped into Al_2O_3, a trigonal host lattice with values of 46° and 116° (19). Nevertheless, the separation of the electronic ground state for $V[(urea)_6]^{3+}$ is larger by approximately 25 % than for the doped oxide, indicating that considering only the metal center and ligator atoms is not sufficient in this case. In addition, Table II shows that the two sets of oxygen atoms related through the trigonal axis are twisted by 7°, leading to a non-centrosymmetric molecular structure. The complete molecular structure is very close to D_3 point group symmetry (16). We attempted AOM calculations for this simple structure and were not able to reproduce the experimental data summarized in Table III by using only the e_σ, e_π, B, C and ζ parameters. An important aspect to the metal ligand bonding of molecules like H_2O or urea is their anisotropic π bonding (2,3). Introducing two e_π parameters, $e_{\pi s}$ and $e_{\pi c}$, does in fact allow us to reproduce the split of the ground state and the emitting state energy, but the spin-allowed absorption maxima are calculated at energies too low by more than 2000 cm^{-1}. This model is therefore also not sufficient. We include a tilt angle Ψ (18) of the ligand π system in our final AOM model. Its value of 27° was estimated from the crystal structure (11). This improved model, with all numerical parameter values given in Table II, leads to a good agreement between observed and calculated energy differences obtained from luminescence, Raman and absorption spectroscopy, as summarized in Table III. The ground state levels are illustrated in the right hand column of Figure 6. It is important to note that the angle is an incomplete description of the metal-ligand geometry: the plane of the ligands is also tilted away from the trigonal axis and the V-O-C angles, implicitly assumed to be 180° for our AOM calculation, vary from 137.0° at 300 K to 133.6° at 90 K (11). Nevertheless, this is the simplest AOM

Table II. Ligand field (AOM) parameters for $V(urea)_6I_3$.

Parameter	Value
e_σ [cm^{-1}]	8448
$e_{\pi s}$ [cm^{-1}]	1858
$e_{\pi c}$ [cm^{-1}]	2803
B [cm^{-1}]	727
C [cm^{-1}]	2470
ζ [cm^{-1}]	16
θ_1, ϕ_1, ψ_1 [°]	55.26, -34.43, 27.0
θ_2, ϕ_2, ψ_2 [°]	55.28, 205.61, 27.0
θ_3, ϕ_3, ψ_3 [°]	55.23, 85.60, 27.0
θ_4, ϕ_4, ψ_4 [°]	124.71, 152.58, -27.0
θ_5, ϕ_5, ψ_5 [°]	124.68, 32.60, -27.0
θ_6, ϕ_6, ψ_6 [°]	124.74, -87.39, -27.0

model that allows us to completely rationalize the spectroscopic data.

An alternative approach to theoretically determine energy differences is provided by advanced electronic structure calculations. We use density functional calculations to determine the orbital energy levels of $V[(urea)_6]^{3+}$, based on its experimental structure. The orbital energies obtained from the DFT calculations (20) are compared to the AOM energies in Table IV. The splitting patterns obtained from both calculations are similar and correspond to an e – a_1 – e pattern (D_3 point group labels). The separation of the e orbitals arising from the t_{2g} (O_h) orbitals is larger by an order of magnitude in the DFT calculation than derived from the spectra with the AOM approach. In contrast, the energy difference between the e and a_1 orbitals from the DFT calculation is smaller by an order of magnitude than the AOM value. The energies of the e orbitals arising from e_g (O_h) are similar, but again the DFT calculation predicts a somewhat larger separation. The overall consistency of these energies indicates that the empirical AOM parameters in Table II are reasonable. The orbitals from DFT clearly show anisotropic interactions with nonzero $e_{\pi s}$ and $\varepsilon_{\pi\chi}$ contributions caused by the orientation of the urea ligands with respect to the vanadium-oxygen bonds. The model calculations lead to insight on the origin of the large ground state splitting observed in Figures 1 and 3, but it is also obvious that DFT calculations alone do not predict correct energy differences.

The results for the doped chloride crystal in Figure 4 illustrate that information can be obtained even from luminescence spectra of very inhomogeneous solids. The sharp peaks correspond to electronic or vibronic origins. From the experimental data, we can assign the bands lower in energy by 151 cm^{-1} and 203 cm^{-1} than the prominent origin at 9497 cm^{-1} as vibronic origins because hot bands at similar energy differences of 117 cm^{-1} and 210 cm^{-1} are observed. These energies correspond to ungerade parity enabling modes in the ground and emitting states, as it is unlikely that the singlet emitting state and the triplet ground state have such similar spin-orbit and low-symmetry levels. The energy differences between the remaining sharp transitions are much larger than the spin-orbit splittings for octahedral $[VCl_6]^{3-}$ luminophores, and the pattern deviates

Table III. Observed and calculated energies of electronic states of $V(urea)_6I_3$. Calculated energies were obtained with the AOM and the parameters in Table II.

State, labels: D_3 with spin-orbit coupling, D_3 (O_h) without spin-orbit coupling	Calculated energy [cm^{-1}]	Observed energy [cm^{-1}]
A_1, $^3A_2$ ($^3T_{1g}$)	0	
E, $^3A_2$ ($^3T_{1g}$)	6	6[a]
E, ^3E ($^3T_{1g}$)	1358	
E, ^3E ($^3T_{1g}$)	1476	1392[b]
A_2, ^3E ($^3T_{1g}$)	1574	
A_1, ^3E ($^3T_{1g}$)	1589	
E, ^1E ($^1T_2$)	9844	9928[b,c]
E, ^1E (^1E)	11306	
A_1, $^1A_1$ ($^1T_2$)	11470	
A_2, $^3A_1$ ($^3T_{2g}$)	14987	15576[c]
E, $^3A_1$ ($^3T_{2g}$)	14995	
A_2, ^3E ($^3T_{2g}$)	15588	16518[c]
A_1, ^3E ($^3T_{2g}$)	15590	
E, ^3E ($^3T_{2g}$)	15630	
E, ^3E ($^3T_{2g}$)	15668	
A_1, $^1A_1$ ($^1A_{1g}$)	22158	21638[c]
A_1, $^3A_2$ ($^3T_{1g}$)	24588	24764[c]
E, $^3A_2$ ($^3T_{1g}$)	24598	
A_2, ^3E ($^3T_{1g}$)	25148	
A_1, ^3E ($^3T_{1g}$)	25166	
E, ^3E ($^3T_{1g}$)	25219	
E, ^3E ($^3T_{1g}$)	25271	

[a] Luminescence for $V(urea)_6(ClO_4)_3$ (7)
[b] Luminescence and electronic Raman, this report
[c] Polarized absorption (16)

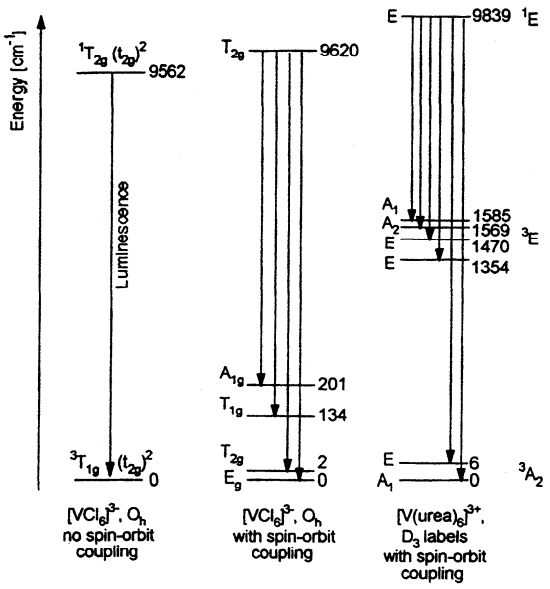

Figure 6. Ground state splittings and emitting state energies for six-coordinate vanadium(III) complexes. The values for $[VCl_6]^{3-}$ are taken from the literature (6). The values for $[V(urea)_6]^{3+}$ are determined from the spectra reported in this work with the parameters given in Table II.

Table IV. Calculated orbital energies. Comparison of the angular overlap model (AOM) and density functional (DFT) calculations. The AOM energies are calculated with the parameter values in Table II, except $\xi = 0$.

Orbital, D_3 (O_h) labels	AOM energy [cm^{-1}]	DFT energy [cm^{-1}]
e (t_{2g})	0	0
e (t_{2g})	2	51
a_1 (t_{2g})	1343	187
e (e_g)	16260	17650
e (e_g)	16260	17726

strongly from the 2:1 splitting expected for a perfect octahedral coordination, as illustrated in the middle column of Figure 6 (6). The energies of the sharp bands again suggest a low symmetry coordination environment. This conclusion is further corroborated by the broad electronic transition to higher-energy ground state components approximately 1000 cm^{-1} below the highest energy transition. This electronic transition shows a vibronic progression with an interval of 300 cm^{-1}, as indicated in Figure 4, suggesting that the structure of the $[VCl_6]^{3-}$ molecular unit is different in the low and high energy ground state levels. The structural differences can occur along totally symmetric normal modes and along Jahn-Teller active modes. The resolution of the spectra in Figure 4 does not allow us to identify all modes, but a contribution from the totally symmetric V–Cl stretching mode is likely. The experimental spectra are not sufficiently resolved to assign modes and we do not attempt to estimate the structural differences. Sophisticated *ab initio* calculations have been carried out on V^{3+} ions doped into a variety of fluoride, chloride and bromide elpasolites (21). They lead to energies of the singlet emitting state within 500 cm^{-1} of the experimental value, a very high precision that is nevertheless not sufficient to attempt an interpretation of the rich splitting pattern observed in Figure 4.

Some persisting instrumental limits of luminescence spectroscopy are illustrated in Figure 5 by the spectroscopic results for vanadium(III) doped into alums. These spectra show only a single band, the highest energy origin, corresponding to the most intense band in the spectra shown in Figures 1 and 4. All other bands of the vanadium(III) alums are expected to be much weaker by qualitative comparison with the spectra analyzed in the preceding sections, and they are too weak to be detected with our instruments. The results presented in Figure 5 allow us to determine the energy of the emitting state, providing complementary information on the electronic structure of these solids. EPR and electronic Raman are the spectroscopic techniques that have been most often used to characterize the ground state of vanadium(III) alums (2,3), but it is important to realize that luminescence measurements are possible and lead to additional insight. From the spectra in Figure 5b, it is easy to distinguish between the two similar ligands D_2O and H_2O by the shift of the luminescence band. The $[V(D_2O)_6]^{3+}$ emission appears 34 cm^{-1} higher in energy that the corresponding band from the aquo analogs. This value is surprisingly similar to the 49 cm^{-1} shift observed for the lowest-energy origin in the near-infrared absorption spectra of $[Ni(H_2O)_6]^{2+}$ and $[Ni(D_2O)_6]^{2+}$ (22), even though the latter transition involves electronic states arising from two different electron configuration, a situation where a deuteration effect larger than for the spin flip transitions in Figure 5 is expected. This difference is illustrated by the absorption spectra of $Cs_2[CrCl_2(H_2O)_4]Cl_3$ and its deuterated analog. The origin of the broad transition to the lowest energy quartet state, involving a change of electron configuration, shifts by 127 cm^{-1} upon deuteration, whereas the origin of the transition to the lowest energy doublet state, a spin flip transition, shifts by only 3 cm^{-1} (12). The spectra in Figure 5b show therefore an unusually large shift due to deuteration, possibly a manifestation of the effect of deuteration on hydrogen bonds throughout the crystal.

In summary, the most important aspects of the near-infrared luminescence spectra of low-symmetry vanadium(III) complexes are presented and compared here. A variety of intricate effects contribute to the observed splitting patterns. Near-infrared luminescence spectroscopy is shown to be a widely applicable and important technique for the characterization of their ground and low-energy excited electronic states.

Acknowledgement

We thank Philip W. L. Tregenna-Piggott (Universität Bern, Switzerland) for the crystals of $CsAl(SO_4)_2 \cdot 12D_2O$ doped with $[V(D_2O)_6]^{3+}$. Financial support from the Natural Sciences and Engineering Research Council (Canada) is gratefully acknowledged.

References

1. D.R. Gamelin and H.U. Güdel, *Acc. Chem. Res.*, **33**, 235 (2000).
2. P.L.W. Tregenna-Piggott, S.P. Best, H.U. Güdel, H. Weihe and C.C. Wilson, *J. Sol. Stat. Chem.*, **145**, 460 (1999).
3. D. Spichiger, G. Carver, C. Dobe, J. Bendix, P.L.W. Tregenna-Piggott, R. Meier and G. Zahn, *Chem.Phys.Lett.*,**337**, 391 (2001).
4. O.S. Wenger and H.U. Güdel, *Inorg. Chem.*, **40**, 5747 (2001).

5. O.S. Wenger and H.U. Güdel, *J. Phys. Chem. B*, **105**, 4181 (2001).
6. C. Reber and H.U. Güdel, *J. Lumin.*, **42**, 1 (1988).
7. C.D. Flint and P. Greenough, *Chem. Phys. Lett.*, **16**, 369 (1972).
8. Z. Goldschmidt, W. Low and M. Foguel, *Phys. Lett.*, **19**, 17 (1965).
9. L A. Riseberg, H.W. Moos and W.D. Partlow, *IEEE J. Quant. Electr.*, **QE-4**, 609 (1968).
10. B. Champagnon and E. Duval, *J. de Phys. Lett.*, **38**, 299 (1977).
11. B.N. Figgis and L.G.B. Wadley, *J. Chem. Soc., Dalton Trans.*, 2182 (1972).The coordinates of V^{3+} in Table 2(a) of this reference are (0, 0, 1/4) in order to be consistent with the bond lengths and angles in Table 2(b).
12. G. Bussière, R. Beaulac, B. Cardinal-David and C. Reber, *Coord. Chem. Rev.*, **219-221**, 509 (2001).
13. C. Reber, H.U. Güdel, G. Meyer, T. Schleid and C.A. Daul, *Inorg. Chem.*, **28**, 3249 (1989).
14. S.M. Jacobsen, W.E. Smith, C. Reber and H.U. Güdel, *J. Chem. Phys.*, **84**, 5205 (1986).
15. C. Reber and H.U. Güdel, *Chem. Phys. Lett.*, **154**, 425 (1989).
16. R. Dingle, P.J. McCarthy and C.J. Ballhausen, *J. Chem. Phys.*, **50**, 1957 (1969).
17. Adamsky, H. *AOMX - an angular overlap program*; Institut für Theoretische Chemie, Heinrich-Heine-Universität Düsseldorf: Düsseldorf, Germany, 1995. The program is available at http://www.theochem.uni-duesseldorf.de/Computing/Progs/aomx/Welcome.html
18. C. E. Schäffer, *Struct. Bond.*, **5**, 68 (1968).
19. L. Pauling and S. B. Hendricks, *J. Am. Chem. Soc.*, **47**, 781 (1925).
20. MacSPARTAN Pro, Version 1.0.4, Wavefunction, Inc., 18401 Von Karman Ave., Suite 370, Irvine, CA 92612,U.S.A. The SVWN density functional approach and DN^{**} basis set were used. The molecular symmetry option was enabled and the MAXCYCLE=99, BADSTEPS=35, DIIS=3, CONVERGE=0.02 settings were specified. It is interesting to note that a significantly better numerical convergence was achieved for a model complex with identical atomic coordinates and a metal center with the d^3 electron configuration, leading to an orbitally nondegenerate ground state. This observation illustrates the inherent challenges of characterizing the orbitally degenerate ground state for the d^2 electron configuration.
21. A.Al-Abdalla, L. Seijo and Z. Barandiarán, *J. Mol. Struct. (Theochem)*, **451**, 135 (1998).
22. J. Landry-Hum, G. Bussière, C. Daniel and C. Reber, *Inorg. Chem.*, **40**, 2595 (2001).